THE JOURNAL OF PHYSICAL CHEMISTRY A

Article

pubs.acs.org/JPCA

Heterogeneous Reactions of Epoxides in Acidic Media

Vinita Lal,[†] Alexei F. Khalizov,[†] Yun Lin,[†] Maria D. Galvan,[‡] Brian T. Connell,[‡] and Renyi Zhang*[,†,‡]

[†]Department of Atmospheric Sciences and [‡]Department of Chemistry, Texas A&M University, College Station, Texas 77843, United States

ABSTRACT: Epoxides have recently been identified as important intermediates in the gas phase oxidation of hydrocarbons, and their hydrolysis products have been observed in ambient aerosols. To evaluate the role of epoxides in the formation of secondary organic aerosols (SOA), the kinetics and mechanism of heterogeneous reactions of two model epoxides, isoprene oxide and α-pinene oxide, with sulfuric acid, ammonium bisulfate, and ammonium sulfate have been investigated using complementary experimental techniques. Kinetic experiments using a fast flow reactor coupled to an ion drift-chemical ionization mass spectrometer (ID-CIMS) show a fast irreversible loss of the epoxides with the uptake coefficients (γ) of $(1.7 \pm 0.1) \times 10^{-2}$ and $(4.6 \pm 0.3) \times 10^{-2}$ for isoprene oxide and α-pinene oxide, respectively, for 90 wt % H_2SO_4 and at room temperature. Experiments using attenuated total reflection—Fourier transform infrared spectroscopy (ATR-FTIR) reveal that diols are the major products in ammonium bisulfate and dilute H_2SO_4 (<25 wt %) solutions for both epoxides. In concentrated H_2SO_4 (>65 wt %), acetals are formed from isoprene oxide, whereas organosulfates are produced from α-pinene oxide. The reaction of the epoxides with ammonium sulfate is slow and no products are observed. The epoxide reactions using bulk samples and Nuclear Magnetic Resonance (NMR) spectroscopy reveal the presence of diols as the major products for isoprene oxide, accompanied by aldehyde formation. For α-pinene oxide, organosulfate formation is observed with a yield increasing with the acidity. Large yields of organosulfates in all NMR experiments with α-pinene oxide are attributed to the kinetic isotope effect (KIE) from the use of deuterated sulfuric acid and water. Our results suggest that acid-catalyzed hydrolysis of epoxides results in the formation of a wide range of products, and some of the products have low volatility and contribute to SOA growth under ambient conditions prevailing in the urban atmosphere.

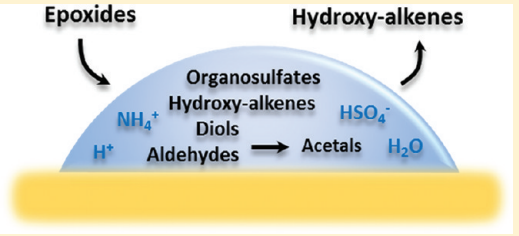

1. INTRODUCTION

As discussed in a seminal paper by Ravishankara,[1] heterogeneous and multiphase reactions play a central role in partitioning of chemical species in the troposphere, including the gas-to-particle conversion process of organic compounds. Globally large quantities of volatile organic compounds (VOCs) are emitted into the atmosphere from biogenic and anthropogenic sources. In the atmosphere, VOCs are photochemically oxidized to form a broad range of products,[2−4] some of which can participate in a number of physical and chemical processes leading to formation of secondary organic aerosols (SOA).[5,6] Because organic aerosols constitute a significant fraction of the tropospheric aerosol loading, the understanding of the SOA formation mechanism is crucial for accurate assessment of the impacts of atmospheric aerosols on air quality, human health, and climate forcing.[7−9] The major SOA formation pathways currently identified include condensation of low-volatility organics, gas-to-particle partitioning of semivolatile (SVOC) and intermediate volatility (IVOC) organics,[10,11] and heterogeneous chemical reactions on pre-existing particles.[12−16] Furthermore, organic compounds have been suggested to play an important role in the nucleation and growth of nanoparticles.[15,17−21]

Although both biogenic and anthropogenic sources contribute to the tropospheric SOA loading, the SOA precursors from biogenic VOCs (BVOCs) outnumber those from anthropogenic VOCs by a large margin.[6,22] Isoprene and monoterpenes, constituting the largest fraction of the BVOCs, are thought to contribute significantly to SOA formation.[23,24] Laboratory studies indicate that in the presence of acidic seeds the SOA production from photo-oxidation of isoprene and monoterpenes is enhanced and significant quantities of 2-methyltetrols[25] and organosulfates[26,27] are formed in the particle phase. Several studies have shown organosulfates to be an important constituent of ambient SOA.[26−35] Because direct reaction of alcohols with sulfuric acid to form sulfate esters is not kinetically feasible,[36] substantial research effort has been made in identifying other oxidized organic species that produce organosulfates. Recent chamber experiments have shown that organosulfates are formed upon reactive uptake of gas-phase epoxides (α- and β-pinene oxides) by acidic aerosols.[37] The kinetics and mechanism of acidic hydrolysis of several different epoxides have been investigated in dilute bulk solutions.[38−41] Organosulfate formation has been found to be kinetically favorable for epoxides compared to other oxidized products, such as alcohols, and lead to the formation of low-volatility species.[38]

In earlier studies, formation of epoxides has been observed in high yields in gas-phase oxidation of alkenes by $O(^3P)$[42−44]

Special Issue: A. R. Ravishankara Festschrift

Received: November 23, 2011
Revised: February 2, 2012
Published: February 6, 2012

Table 1. Saturation Vapor Pressure of Isoprene Oxide and α-Pinene Oxide at Different Temperatures[a]

	vapor pressure (Torr)			Antoine equation constants	
epoxide	298 K	273 K	193 K	*A*	*B*
isoprene oxide	79.7 ± 1.61 (102)	24.4 ± 1.25	0.02 ± 0.007	19.905	−4592.3
α-pinene oxide	0.82 ± 0.03 (0.8)				

[a]Antoine equation constants for isoprene oxide are provided. Values in parentheses are estimated using ACD Labs software

and in minor quantities during oxidation by ozone[43,44] and NO_3.[45−48] Recently, epoxides have been identified as intermediate products in the photo-oxidation of isoprene by OH under low NO_x conditions[49] and the presence of hydrolysis products of isoprene-derived epoxydiols in ambient aerosols has also been reported.[30] The crucial role of epoxydiols as the reactive intermediates in the formation of SOA from isoprene has been clearly shown in recent chamber studies.[35,50]

In this study, the heterogeneous reactions of isoprene oxide and α-pinene oxide have been investigated using several complementary analytical techniques to assess the role of biogenic epoxides as the SOA precursors under different reaction conditions. The kinetic and product studies were conducted using sulfuric acid, ammonium bisulfate, and ammonium sulfate as the condensed media and using micrometer-sized droplets and bulk solution to obtain a better understanding of the mechanisms by which epoxides react under atmospheric conditions.

2. EXPERIMENTAL DETAILS

All the reagents, including H_2SO_4 (95−98%, ACS reagent grade), D_2SO_4 (96−98 wt % in D_2O), D_2O (standard), isoprene oxide (2-methyl-2-vinyl oxirane, 95%), and α-pinene oxide (97%), were purchased from Sigma-Aldrich. Deionized water (18 mΩ·cm) used for dilutions was produced using a Barnstead E-Pure water system.

2.1. Vapor Pressure Measurements. The equilibrium vapor pressures over bulk samples of isoprene oxide and α-pinene oxide were measured using a vacuum manifold equipped with a capacitance gauge (MKS Baratron, 0−10 Torr, model 622A11TAE) and connected to an oil-sealed vacuum pump. A small volume of liquid epoxide was placed in a glass container connected to the manifold. Before measurements, the epoxide in the container was purified from volatile impurities using a standard freeze-and-thaw procedure. The manifold was then disconnected from the vacuum pump, the container was immersed in a cooling bath maintained at a required temperature, and the epoxide vapor was allowed to reach equilibrium in the manifold. The measurement continued until the epoxide in the container ceased to boil and the equilibrium vapor pressure of the epoxide was established, as indicated by a constant pressure reading on the pressure gauge at a specific temperature. The container temperature was maintained constant using several cooling baths, that is, an ice−water mixture at 273 K, a mixture of dry ice and ethanol at 193 K, and a eutectic mixture of $CaCl_2$ and water chilled by liquid nitrogen to 233 K.

Table 1 shows equilibrium vapor pressures of α-pinene oxide at room temperature and isoprene epoxide at several different temperatures. For isoprene oxide, the experimental temperature-dependent data were used to derive the *A* and *B* parameters of the modified Antoine equation,

$$\ln(P/P_o) = A - \frac{B}{T}$$

where *P* is the equilibrium vapor pressure, P_o is the reference pressure (1 Torr), and *T* is the temperature (K). The vapor pressures measured at room temperature are in agreement with those predicted by ACD (Advanced Chemistry Development) Laboratories software.

2.2. Uptake Rate Experiments. The uptake experiments were carried out in a low-pressure laminar flow reactor coupled to an ion drift—chemical ionization mass spectrometer (ID-CIMS), as described previously.[12,13,51−55] Aqueous sulfuric acid solution in a Pyrex glass trough was placed inside a 50 cm long Pyrex flow reactor. The epoxide−He gas mixture was introduced to the reactor through a movable glass injector. The pressure inside the flow reactor was maintained at around 1.5 Torr. The temperature of the flow reactor was controlled by passing SYLTHERM fluid through the outer jacket using Neslab UT-80 circulator. All carrier gas flows were monitored using calibrated electronic mass flow meters (Millipore Tylan 260 Series).

A 2 L glass bulb containing epoxide vapor (100 ppm) in He was prepared by a two-step dilution process.[51] The partial pressure of epoxide in the reactor was 10^{-6}−10^{-7} Torr. Sulfuric acid solutions of known concentrations (66, 75, 85, and 90 wt %) were prepared from 96 to 98% H_2SO_4 stock solution using deionized water (18 mΩ cm). Before and after each experiment, the acid composition was checked by titration with standard 0.1 N NaOH solution. As the vapor pressure of water above sulfuric acid solutions increases with increasing temperatures and decreasing concentrations,[56−58] water vapor was added to He in the flow tube to reduce changes in the acid composition. The temperature range for the uptake experiments was regulated between 243 and 298 K.

The epoxides were detected via chemical ionization using H_3O^+ and O_2^- as reagent ions. The ion−molecule reactions involved proton transfer and association, respectively.

$$H_3O^+ + X \rightarrow XH^+ + H_2O$$

$$X + O_2^- \rightarrow X \bullet O_2^-$$

H_3O^+ was used to monitor the ions *m*/*z* 85 (protonated epoxide) and *m*/*z* 43 (fragment $C_2H_3O^+$) for isoprene oxide and *m*/*z* 43 and *m*/*z* 93 (fragments from epoxide) for α-pinene oxide.[59] With O_2^-, the ions monitored were *m*/*z* 116 ($C_5H_{10}O{\cdot}O_2^-$) for isoprene oxide and *m*/*z* 184 ($C_{10}H_{16}O{\cdot}O_2^-$) for α-pinene oxide.

The reaction between epoxides and sulfuric acid was studied by exposing a certain length of the acid surface to epoxide vapors by stepwise retracting the injector tip upstream of the acid surface and simultaneously monitoring the epoxide signal. The uptake coefficient γ of epoxide over H_2SO_4 was calculated from the change in the epoxide signal on exposure to acid and exposed length of the acid surface, as described previously.[51,52]

2.3. ATR-FTIR Experiments. ATR-FTIR studies were performed using the Nicolet Magna 560 spectrometer equipped with a liquid nitrogen cooled MCT detector. The reaction between epoxide and deposited micrometer-sized particles was carried out in a covered multiple reflection horizontal trough

dx.doi.org/10.1021/jp2112704 | J. Phys. Chem. A 2012, 116, 6078−6090

ATR accessory (Pike Technologies) with a ZnSe crystal, located in the sample compartment of the FTIR spectrometer. Sulfuric acid, ammonium bisulfate, and ammonium sulfate particles of a 1−5 μm diameter were deposited on the ATR crystal using a TSI 3076 Constant Output Atomizer.[16] The total mass of deposited particles was ∼30 μg after 2 min exposure, as estimated from Scanning Electron Microscope (SEM) and optical microscope images. A mixed dry and moist nitrogen flow was used to achieve a desired relative humidity (RH) inside the ATR reaction cell and hence to regulate the composition of particles.[16] The relation between concentration of the solute and RH was calculated using water vapor pressure data over aqueous sulfuric acid, ammonium bisulfate, and ammonium sulfate solutions.[60,61] Once a desired composition was achieved, a background spectrum of solid particles or liquid droplets was collected so that after exposure to epoxides the spectra included only the product peaks. Typically, 64 scans were averaged to yield a complete spectrum in the range of 4000−700 cm^{-1}, with a resolution of 2 cm^{-1}. After obtaining a background spectrum, epoxide vapors were passed over the particles in the ATR cell, and spectra were recorded at various time intervals to identify the development of new peaks, characteristic of the reaction products. The initial concentrations of α-pinene oxide and isoprene oxide were measured using a proton transfer reaction mass spectrometer (PTR-MS, Ionicon). A complete experiment included recording of the background spectrum with deposited particles and then collecting a series of spectra as the particle-epoxide reaction progressed.

All ATR-FTIR experiments were carried out at 296 ± 2K. A flow of gaseous epoxide in nitrogen carrier was obtained by collecting vapor from a glass container with corresponding liquid epoxide. For α-pinene oxide, the container was kept at room temperature. For isoprene oxide, the epoxide container was placed in a cooling bath made of a eutectic mixture of 31 wt % $CaCl_2$ in water and frozen using liquid N_2 to keep a temperature of 233 K.[62] At this temperature, the vapor pressure of isoprene oxide was 1.3 Torr. For a complete experiment run time, the temperature of the cooling bath remained constant within ±2 K.

To investigate the changes in size and morphology of particles/droplets upon exposure to epoxides, several measurements were carried out employing an optical microscope. Silicon wafer chips of a 0.9 mm diameter were placed on the ATR crystal, covered with aerosol particles, and the experiment was carried out similarly to all ATR-FTIR experiments. Following the exposure to epoxides, images of the silica chips were taken using the 10× and 50× objectives of the Thermo-Scientific DXR Raman Microscope.

2.4. NMR Experiments. Measurements of the hydrolysis products of epoxides were performed using Inova-300 NMR spectrometer operating at 300 MHz. Three sets of experiments were carried out for each epoxide, using different epoxide/D_2SO_4 ratios. For the first set, 25 μL of epoxide was added to 5 mL of D_2SO_4/D_2O solution of different concentrations, similar to previous studies.[36,38,39] For the second set, 32 μL of epoxide was added to 2 mL of D_2SO_4/D_2O solution of different concentrations. For the third set, 100 μL of epoxide was added to 1 mL of 5 wt % D_2SO_4 in D_2O. All D_2SO_4 solutions were prepared using commercially available D_2SO_4 (96−98%, Sigma-Aldrich) diluted with D_2O. The acid solution was mixed with epoxide and allowed to stand for 5 min. The solution was then transferred to a 5 mm diameter NMR tube and inserted into the spinner. All reaction mixtures were monitored at 296 ± 2 K.

3. RESULTS

3.1. Uptake Experiment. Figure 1a shows the temporal profile of the mass spectrometer signal corresponding to isoprene oxide−O_2^- ion for an uptake experiment carried out at 298 K with 90 wt % H_2SO_4. Epoxide was passed through the movable injector and the signal was monitored to establish a steady-state flow downstream of the trough containing acid. The injector was pulled upstream to expose a certain length of the acid to epoxide. On exposure, the epoxide was taken up by the acid, as indicated by a drop in the epoxide signal. There was no recovery of the signal over the time scale of exposure. When the tip of injector was pushed back downstream the acid surface, the epoxide signal fully recovered to its original level. The absence in the signal recovery while the injector was retracted upstream of the trough and the lack of the desorption peak upon returning the injector downstream indicated that the reaction between epoxide and sulfuric acid was irreversible.[15,51] Similar behavior was observed for α-pinene oxide, also suggesting irreversible uptake. The first-order decay of the epoxide signal was plotted against the reaction distance for each uptake

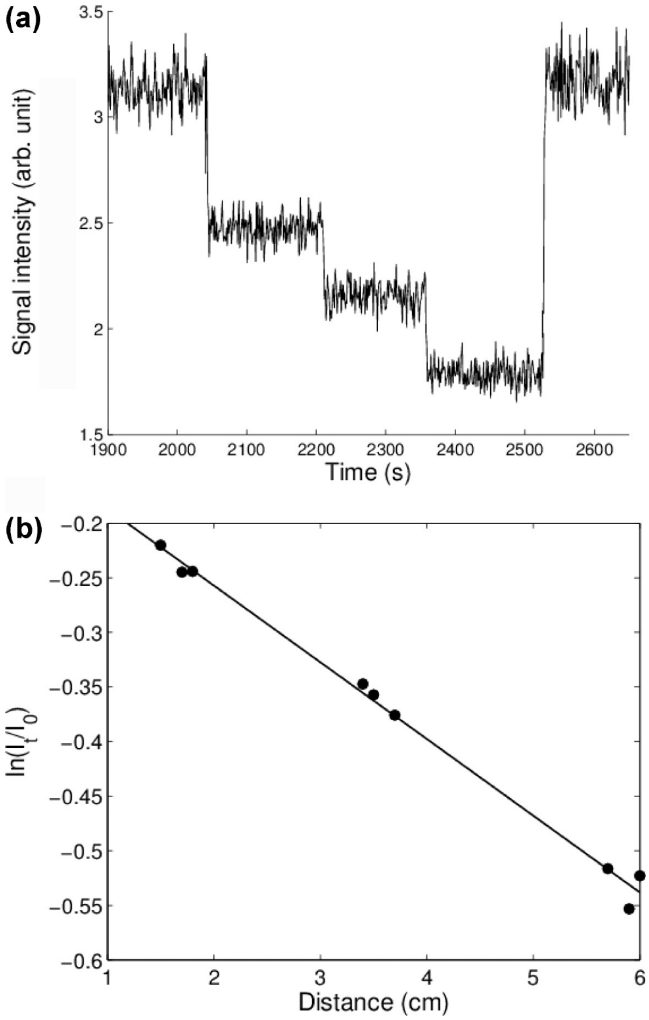

Figure 1. (a) Temporal profile of m/z 116 representing the attachment ions of isoprene oxide with O_2^- on 90 wt % H_2SO_4. The temperature is 298 K, pressure is 1.68 Torr, and gas velocity is 664 cm s^{-1}. Steps in the signal correspond to 1.7, 3.5, and 5.9 cm length of exposed sulfuric acid surface. (b) Logarithm of the normalized is isoprene oxide signal as a function of injector position for the data shown in (a).

dx.doi.org/10.1021/jp2112704 | J. Phys. Chem. A 2012, 116, 6078−6090

experiment, as shown in Figure 1b. The first order rate constants were determined from the slope of the linear regression fit to the data set, and the uptake coefficients were calculated from the obtained first-order rate constants as described previously.[51,63] The uptake coefficients for isoprene oxide and α-pinene oxide at 298 K and on 90 wt % H_2SO_4 solution are $(1.7 \pm 0.1) \times 10^{-2}$ and $(4.6 \pm 0.3) \times 10^{-2}$, respectively (Table 2).

Table 2. Uptake Coefficients of Isoprene Oxide and α-Pinene Oxide on 90 wt % H_2SO_4 at 298 K

	uptake coefficient, $\gamma \times 10^2$	
run #	α-pinene oxide	isoprene oxide
1	4.3	1.76
2	4.9	1.86
3	4.5	1.67
4		1.56
average	4.6 ± 0.3	1.7 ± 0.1

At room temperature, the saturation vapor pressure of water over less concentrated H_2SO_4 solutions (e.g., 0.3 Torr above 75 wt % H_2SO_4) was sufficiently high that the uptake became largely diffusion-limited.

Additional experiments were carried out at lower temperatures using more dilute H_2SO_4 solutions. However, no apparent loss or sometimes even an increase in the epoxide signal was observed upon exposure to the acid solution surface, indicating possible interference from other chemical species to the epoxide signal detected by ID-CIMS under those experimental conditions. Such interference could be caused by formation of volatile products from the heterogeneous reaction between epoxide and sulfuric acid that subsequently evaporated from the solution. For example, some of the products of epoxide hydrolysis, namely aldehydes and hydroxyl-alkenes, may produce molecular ions and/or ion fragments with m/z identical to that of the parent epoxide. The interference was observed for both epoxides, and the reagent ions employed in this study could not distinguish between the epoxide and the interfering species. Therefore, no uptake coefficients could be obtained from lower temperature experiments using dilute H_2SO_4.

3.2. ATR-FTIR. ATR-FTIR spectroscopy was used to identify the reaction products formed upon the uptake of epoxides by H_2SO_4, NH_4HSO_4, and $(NH_4)_2SO_4$. These products were characterized on the basis of absorption features corresponding to different functional groups that appeared and evolved on exposing the epoxide to particles of known composition. For both isoprene oxide and α-pinene oxide, experiments were carried out at different RH and using different epoxide concentrations.

Figure 2 shows the ATR-FTIR spectra for products of the isoprene oxide and α-pinene oxide reactions with H_2SO_4 microdroplets at different RH. Detailed peak assignment in the fingerprint region is provided in Tables 3 and 4. All peaks were identified with the aid of the spectral reference handbook.[64] For α-pinene oxide reaction with H_2SO_4, as shown in Figure 2a–c, the strong broad peak at 3350 cm^{-1} is assigned to the O–H stretch. The intensity of this peak is reduced with decreasing RH. The peaks in the region 3000–2800 cm^{-1} are due to C–H stretch vibrations. The C–H peaks observed under all RH conditions are at similar frequencies, showing the carbon backbone preserved. The fingerprint region is complicated due to the presence of several overlapping peaks from different functional groups. The region at 1400–1300 cm^{-1} includes contributions both from the carbon ring as well as alcohol groups. At 84% RH, the strong peaks at 1136 and 1037 cm^{-1} represent the C–O stretch for tertiary and secondary alcohols, respectively. Peaks in the region 900–800 cm^{-1} represent C–C–O stretch for secondary alcohol group and in the region 800–750 cm^{-1} for tertiary alcohol group. These peaks indicate the presence of a diol product. At 9% RH, the peak at 1037 cm^{-1} is replaced by a weak broad peak at 1066 cm^{-1}, which is assigned to the SO_2 symmetric stretch and a moderately strong peak at 1194 cm^{-1} corresponding to the SO_2 asymmetric stretch. The asymmetric S–O–C stretching vibration occurs at 872 cm^{-1}, a peak of medium intensity.[64,65] The FTIR spectrum at 42% RH shows the presence of diol and a small amount of sulfate. With decreasing RH (i.e., increasing acidity), the concentration of inorganic sulfate in the solution increases and organosulfates are produced. The decrease in O–H absorbance and hence loss of O–H groups supports this observation. The overall absorbance at 9% RH is very low and increases with increasing RH.

For isoprene oxide, as shown in Figure 2d–f, the peaks in the region around 2978 cm^{-1} are assigned to the C–H stretch of $-CH_3$ group while the peaks ranging between 2919 and 2913 cm^{-1} and 2868–2866 cm^{-1} correspond to the $-CH_2$ asymmetric and symmetric stretch, respectively. The medium sharp peaks at ∼3090 cm^{-1} and the peaks in the range 1000–925 cm^{-1} confirm the presence of the vinyl group. This is also supported by the presence of a peak in the 1680 cm^{-1} range, showing the C=C stretch. A small overtone of the vinylic stretch is observed around 1800 cm^{-1}. The peak at 3460 cm^{-1} observed at 13% RH represents the O–H stretch of the reaction products. This band is dependent on the acidity and the frequency decreases in dilute solution due to increasing in hydrogen bonding. Hence, the O–H stretch peak is at 3372 cm^{-1} in case of 41% RH and 3370 cm^{-1} at 80% RH. Overall, there are significant differences in the intensities and position of peaks produced under the low and high RH reaction conditions. While the O–H stretch vibration intensity in the range 3300–3500 cm^{-1} decreases with decreasing humidity, the intensity of peaks in the region of C–O stretch (1200–1000 cm^{-1}) increases. This can be explained by the formation of different products at lower RH. For 80% RH conditions, strong peaks for alcohol C–O stretching vibrations are observed in the region 1200–1000 cm^{-1}. These frequencies are typical of the tertiary alcohol group. The C–O deformation of tertiary alcohols is assigned to the peaks at ∼790 cm^{-1}. The peaks on the higher end of the frequency range correspond to the presence of a $-CH_3$ group attached to the carbon of C–OH. For the higher RH conditions (80 and 41%), strong peaks are observed at 1058 and 1057 cm^{-1}, representing C–O stretch for primary alcohol group. At 13% RH, however, the peak shifts to a higher frequency and represents a very strong absorption at 1085 cm^{-1}, corresponding to the strong band for C–O–C stretching vibration of acetals. Formation of acetals and increase in carbon chain are also evident from the increased intensities of all the alkyl (C–H) vibrations. The strong peaks in the region 1280–1250 cm^{-1} represent the O–H in-plane deformation. The intensity of these peaks decreases with decreasing humidity.

Experiments employing a range of gas-phase epoxide concentrations were carried out at low RH conditions for both α-pinene oxide (9% RH) and isoprene oxide (13% RH). For both the epoxides, a higher concentration resulted in a higher product yield, but the distributions of products remained unchanged. Figure 3 depicts the integrated absorbance for the C–H stretch plotted as a function of epoxide concentration for a

dx.doi.org/10.1021/jp2112704 | J. Phys. Chem. A 2012, 116, 6078–6090

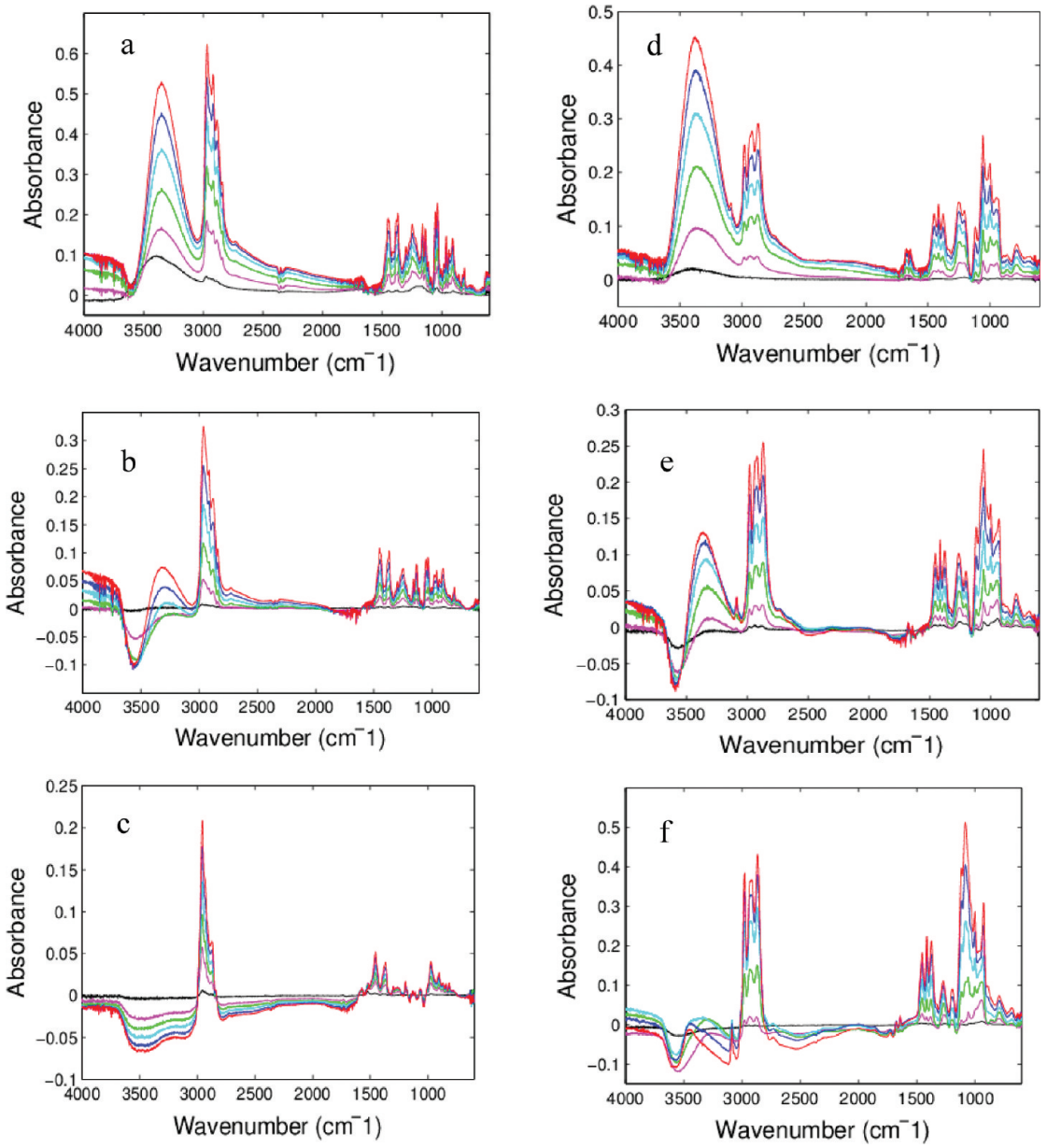

Figure 2. (a–c) ATR-FTIR spectra of the products of α-pinene oxide reaction with H_2SO_4 at (a) 84% RH, (b) 42% RH, and (c) 9% RH. The total experimental run-time is 50 min for each case. (d–f) ATR-FTIR spectra of the products of isoprene epoxide reaction with H_2SO_4 at (d) 80% RH, (e) 40% RH, and (f) 13% RH. The total experimental run-time is 25 min for each case.

Table 3. ATR-FTIR Absorption Frequencies Assigned to the Functional Groups Formed by Acid Hydrolysis of α-Pinene Oxide

	frequencies (cm^{-1})		
assignment of frequency	RH 84%	RH 42%	RH 9%
O–H stretch	3349	3372	not significant
C–O stretch (secondary alcohol/ sulfate*)	1037	1058	1070*
O–H in-plane deformation/sulfate*	1247	1262	1267*, 1194*
C–O stretch (tertiary alcohols)	1135, 1159	1202	1148
S–O stretch			872

Table 4. ATR-FTIR Absorption Frequencies Assigned to the Functional Groups Formed by Acid Hydrolysis of Isoprene Oxide

	frequencies (cm^{-1})		
assignment of frequency	RH 80%	RH 41%	RH 13%
O–H stretch	3372	3372	3460
C–O stretch (primary alcohol/acetal*)	1057	1058	1085*
O–H in-plane deformation	1250	1262	1278
C–O stretch (tertiary alcohols/acetal*)	1205	1202	1193*
C–O deformation for tertiary alcohol	784	787	792

given reaction run-time. For both epoxides, the integrated intensity is linearly proportional to epoxide concentration. This observation is consistent with the first-order reaction rate of acid hydrolysis of epoxides with respect to epoxide concentration.[38,39]

The reactions of epoxides with ammonium sulfate and bisulfate particles were also carried out to investigate the importance of acid catalysis in hydrolysis of epoxides.

dx.doi.org/10.1021/jp2112704 | J. Phys. Chem. A 2012, 116, 6078–6090

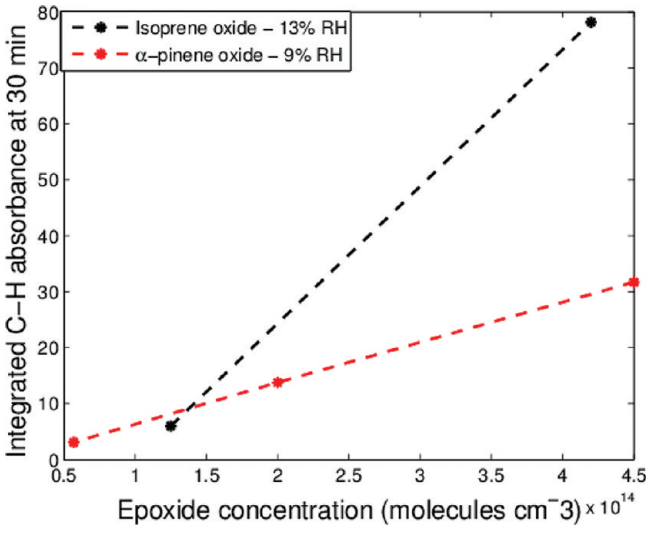

Figure 3. Integrated absorbance for C–H stretch region (3000–2850 cm^{-1}) as a function of epoxide concentration at 9% RH for α-pinene oxide and 13% RH for isoprene oxide reaction with H_2SO_4. The experimental run-time is 30 min for each case.

Ammonium sulfate represents a close to neutral substrate. The reaction of both epoxides with dry and deliquesced ammonium sulfate was slow and no identifiable products were formed in either case, similarly as in previous studies.[38] Slow reaction with ammonium sulfate reflects the importance of acid catalysis in the epoxide hydrolysis. However, exposure of epoxides to ammonium bisulfate results in products that have similar spectra and comparable yields as those obtained in reactions with sulfuric acid at high RH conditions.

3.3. NMR. Bulk experiments were conducted to investigate the effect of the epoxide-to-acid (D_2SO_4) ratios on the distribution and yield of products. Bulk solutions were used because the amount of products formed in the ATR-FTIR experiments using microdroplets was insufficient for NMR analysis. Also, acid concentrations greater than 5 wt % were not used in preparation of the bulk reaction mixtures to avoid generation of heat and formation of a dark brown solution/precipitate. In concentrated acid solutions excessive polymerization and dehydration occurred, making it difficult to obtain NMR spectra of the resulting mixtures. In all experiments, deuterium oxide (D_2O) was used as a solvent for NMR instrument locking purposes and to prevent H/D exchange with D_2SO_4.

The experimental details and the product yields for the reactions of α-pinene oxide with D_2SO_4 are summarized in Table 5. Figure 4 shows the ^1H NMR spectrum for reaction products of α-pinene oxide with 0.7 wt % D_2SO_4, formed in the epoxide to acid ratio of 1:63. Both diol and sulfate ester products are observed. A small peak representing double bond is also identified, showing some dehydration. Peaks at 3.8–4.0 ppm are assigned to the protons attached to carbon with a hydroxyl group and peaks at 5.4–5.6 ppm are assigned to the protons attached to carbon with a sulfate group. The position of the sulfate peak is confirmed by carrying out the reaction of α-pinene oxide with D_2SO_4 (0.1 wt %) and Na_2SO_4 (5 wt %) solutions, similarly as in the previous study on acid hydrolysis of epoxides.[38] The peak at 3.8 ppm represents protons associated with the diol product whereas the peak at 4.0 ppm

Table 5. Product Yields for α-Pinene Oxide Hydrolysis Reaction in D_2SO_4 /D_2O Obtained in NMR Experiments, Using Different Acid to Epoxide Ratios

	products (% yield)			
experimental conditions	diols	hydroxy-sulfate	disulfate	aldehyde
0.02% D_2SO_4/epoxide (63:1)	45	55		
0.3% D_2SO_4/epoxide (63:1)	40	22	38	
0.7% D_2SO_4/epoxide (63:1)	38	27	35	
5% D_2SO_4/epoxide (200:1)	29	26	45	
5% D_2SO_4/epoxide (200:1) diluted with D_2O	37	31	28	4
5% D_2SO_4/epoxide (10:1)	41	16	41	2

represents protons associated with hydroxy-sulfate, with sulfate attached to a tertiary carbon atom. The protons attached to the sulfate functionalized carbon show upfield compared to those corresponding to the hydroxy functionalized carbon.[38−40] The peak at 5.5 ppm is assigned to the protons associated with the secondary carbon atom to which sulfate group is attached. The peak for disulfate product is identified at 5.4 ppm. In experiments with very dilute D_2SO_4, both diol and hydroxyl-sulfate products are shown to form, but in different ratios and no dehydration products are observed. This result is consistent with previous studies on acid hydrolysis of epoxides.[37,38]

For the experiment with a higher epoxide to acid ratio (1:10), aldehyde product is formed with a chemical shift at 9.6 ppm, along with diol and the sulfate ester. This aldehyde may form as a result of rearrangement of α-pinene oxide in the presence of acid, as shown previously.[37] Aldehyde is also formed in small amounts when the epoxide hydrolysis product obtained using 5 wt % D_2SO_4 is diluted 10 times with D_2O. However, in all the reactions, diol represents one of the major products. The sulfate product yield increases with increasing D_2SO_4 concentration. Also, an increase in acid concentration leads to different branching ratios of the hydroxyl-sulfate and disulfate products.

The ^1H NMR spectrum of the reaction mixture of isoprene oxide with 5 wt % D_2SO_4 in the epoxide to acid ratio of 1:200 is shown in Figure 5. In contrast to the previous studies,[39] in which only 1,2-diol was reported, considerable amounts of 1,4-diol and aldehyde are observed in this study. However, similar to the previous studies, no organosulfate formation is detected.[39] For the 1,4-diol product, during hydrolysis, a conjugated carbocation is formed via epoxide ring-opening, and a hydroxyl group is attached to C-4 carbon of the carbocation resonance structure. An allylic rearrangement was confirmed from the peaks at ~4 ppm, which represent the protons attached to C-1 carbon containing hydroxyl groups, and the peak at 5.3 ppm representing hydrogen associated with the double bond. The protons associated with C-1 carbon show upfield in case of 1,4-diol, as compared to 1,2-diol, because of the conjugation with double bond. A small peak at 9.3 ppm is assigned to the aldehyde group. Also, a peak is observed around 7 ppm, which represents a proton attached to the double bonded carbon atom adjacent to the aldehyde group. This suggests that an aldehyde group conjugated to double bond is a favored structure. The previous studies also show that epoxides can form aldehydes in the presence of acid.[66]

Similar products are observed in the experiments using other concentrations and acid-to-epoxide ratios. At low acid concentration (0.7 wt %), aldehyde formation is negligible. Although the ratio of the products varies at a higher epoxide-to-acid ratio,

dx.doi.org/10.1021/jp2112704 | J. Phys. Chem. A 2012, 116, 6078–6090

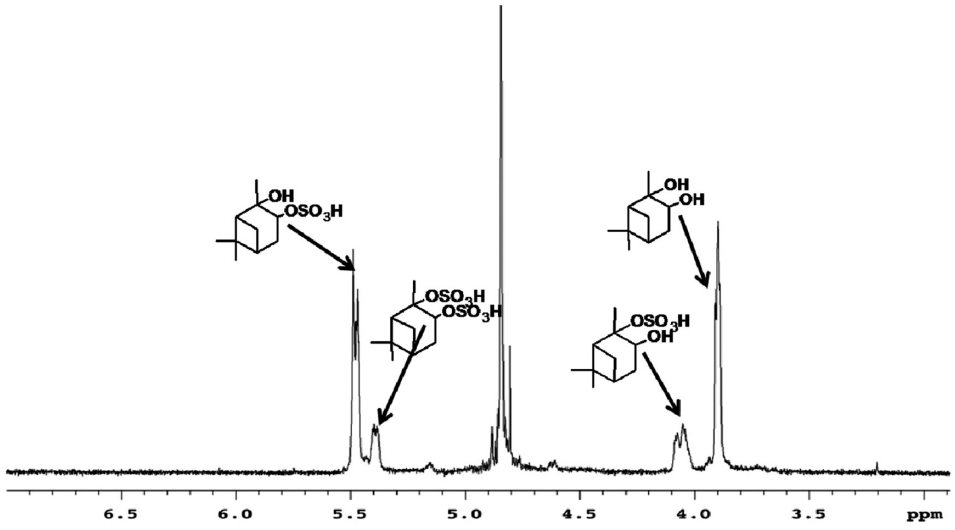

Figure 4. ^{1}H NMR spectrum of α-pinene oxide reaction products in 0.7 wt % D_2SO_4 at 298 K. The chemical shifts depicted are associated with protons attached to carbons with the respective functional groups.

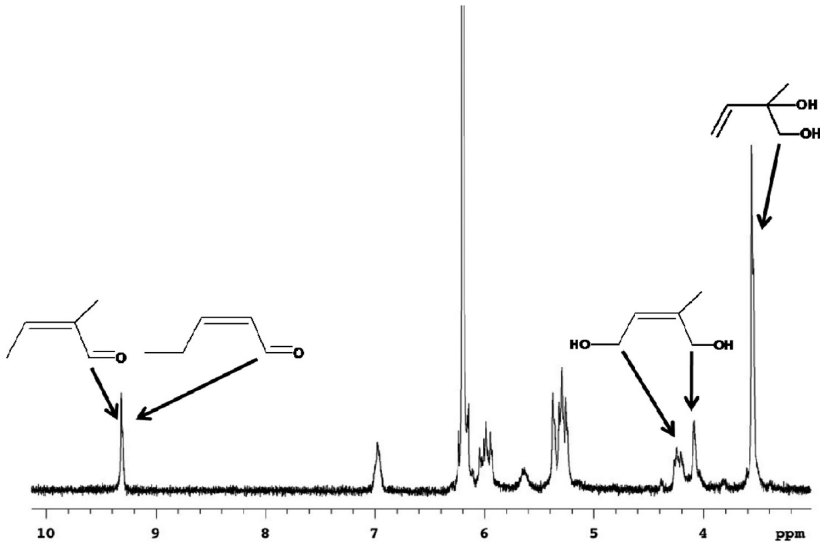

Figure 5. ^{1}H NMR spectrum of isoprene oxide reaction products in 5 wt % D_2SO_4 at 298 K. The chemical shifts depicted are associated with protons attached to carbons with the respective functional groups.

the overall products remain the same. The ratios of products for all the experiments are summarized in Table 6.

Table 6. Product Yields for Isoprene Oxide Hydrolysis Reaction in D_2SO_4/D_2O Obtained in NMR Experiments Using Different Acid to Epoxide Ratios

	products (% yield)		
experimental conditions	1,2-diols	1,4-diols	aldehyde
0.7% D_2SO_4/epoxide (63:1)	80	20	
5% D_2SO_4/epoxide (200:1)	64.5	19.5	16
5% D_2SO_4/epoxide (10:1)	65	32	3

4. DISCUSSION

Using several complementary experimental techniques, we have investigated heterogeneous chemistry of two model epoxides in acidic media, both in bulk solutions and on deposited particles, by measuring the heterogeneous uptake rates and identifying products under different reaction conditions. The mechanisms proposed on the basis of observed reaction products for isoprene oxide and α-pinene oxide are shown in Schemes 1 and 2, respectively. It should be pointed out that in the present work isoprene oxide is used as a surrogate to gain insight into the heterogeneous reaction mechanisms of epoxydiols (IEPOX), which have been identified as key gas-phase reactive intermediates of isoprene oxidation under the low-NO limit.[49,50] α-Pinene oxide is formed in the atmosphere at about 2% yield upon ozonolysis of α-pinene,[42] and our results indicate that corresponding organosulfates and hydroxyl organosulfates, previously observed in ambient aerosols,[27] may be formed via fast acidic hydrolysis of α-pinene oxide in addition to significantly slower reaction involving direct esterification of diols by sulfuric acid.

In an acidic environment, protonation of epoxides (1-a and 1-b) proceeds either as an SN1 pathway via the carbocation intermediate (1-b and 2-b) or as a modified SN2 pathway, where the nucleophile attacks the protonated epoxide (1-c and 2-c) and the C−O bond of epoxide is preferably cleaved over

dx.doi.org/10.1021/jp2112704 | J. Phys. Chem. A 2012, 116, 6078−6090

Scheme 1

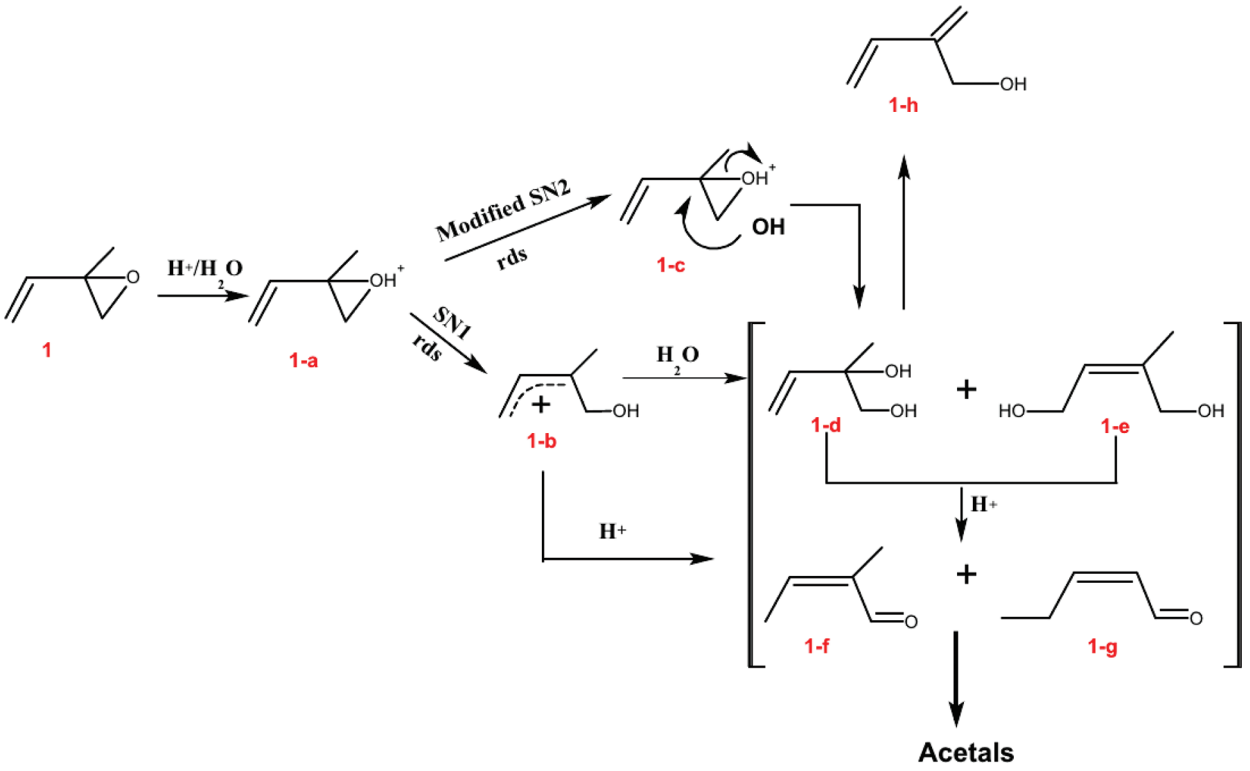

the bond formation between the nucleophile and the protonated carbon. The formation of intermediates (1-b/2-b and 1-c/2-c) from the protonated epoxide (1-a/2-a) corresponds to the rate-limiting steps for the individual reactions. Depending on the intermediate (conjugate acid, 1-a/2-a), different products can form under different acidity conditions. According to the previous studies, the major products of acidic hydrolysis of epoxides are vicinal diols.[37−39] The other products that have been identified in several earlier studies using H_2SO_4 as the reactant are sulfate esters.[37,38] In this study, hydroxy products are observed in the acid hydrolysis of both isoprene oxide and α-pinene oxide (1-d, 1-e, 2-d), while sulfate esters are formed only in the hydrolysis of α-pinene oxide (2-e, 2-f, 2-g). In the case of isoprene oxide, aldehydes are shown to form (1-f, 1-g) that can further react with hydroxy products to form acetals.

4.1. Isoprene Oxide. As shown in Scheme 1, the acidic hydrolysis of isoprene oxide follows either SN1 or modified SN2 pathway to form the products represented by structures 1-d to 1-h. Based on the dominance of the 1,2-diol product, a modified SN2 mechanism has been suggested as the favorable pathway in the previous studies.[67] However, in our study a significant formation of 1,4-diol product is also observed because the presence of methyl group at C-2 carbon and conjugation of the carbocation with the double bond make the SN1 pathway favorable. In the presence of high acid concentration, aldehydes are formed either from the dehydration of these hydroxy-products, or directly from the carbocation 1-b. Epoxides and alcohols in the presence of acid protonate and form a carbocation (mostly secondary or tertiary), which rearranges into an aldehyde.[66,68] Aldehyde formation is evident indirectly in the uptake experiments using ID-CIMS but directly in the NMR studies. The aldehydes can react with the diols to form acetals, which are observed in the ATR-FTIR experiments at low RH, that is, at high acid concentrations. Formation of a hydroxy-alkene is also proposed, as supported from the evidence provided by the previous studies, showing that secondary and tertiary alcohols dehydrate in the presence of acid to form alkenes.[36,69]

The uptake experiments using ID-CIMS show an irreversible heterogeneous reaction of isoprene oxide with H_2SO_4. Because the kinetic measurements were limited to experiments performed using high acid concentration at room temperature due to interference to the epoxide signal, no definite conclusion can be made regarding the effect of temperature and acid concentration on the reaction rate and mechanism, that is, whether the reaction is partially reversible at lower temperatures and acid concentrations. Changes in the uptake behavior at different acid concentrations and temperatures have been reported previously for heterogeneous reaction of alcohols with sulfuric acid solutions.[12] The interference observed in our experiments at lower temperatures ($\leq$283 K) most likely originates from volatile products formed in the heterogeneous reaction of epoxide with sulfuric acid solution. Apparently, the product that interference with the isoprene oxide signal may be ionized effectively, leading to interference with the epoxide ion signal. Since the ion from interfering product has a similar m/z as that of the ion from parent epoxide, the volatile product is interpreted as either an aldehyde (1-f, 1-g) or a hydroxy alkene (1-h). Both species produce molecular ions and ion fragments of the same m/z as the original epoxide under chemical ionization schemes employed in our study, and this interpretation is supported by comparing the ion−molecule reaction rate constants of epoxides and aldehydes/hydroxy-alkenes.[70,71] The formation of volatile aldehydes and hydroxy-alkenes becomes a preferred reaction path at lower temperatures. At room temperature (~298 K), aldehydes, if formed, can react with hydroxy-alkenes to form acetals/hemiacetals or undergo aldol condensation, both processes forming higher molecular weight products of

dx.doi.org/10.1021/jp2112704 | J. Phys. Chem. A 2012, 116, 6078−6090

Scheme 2

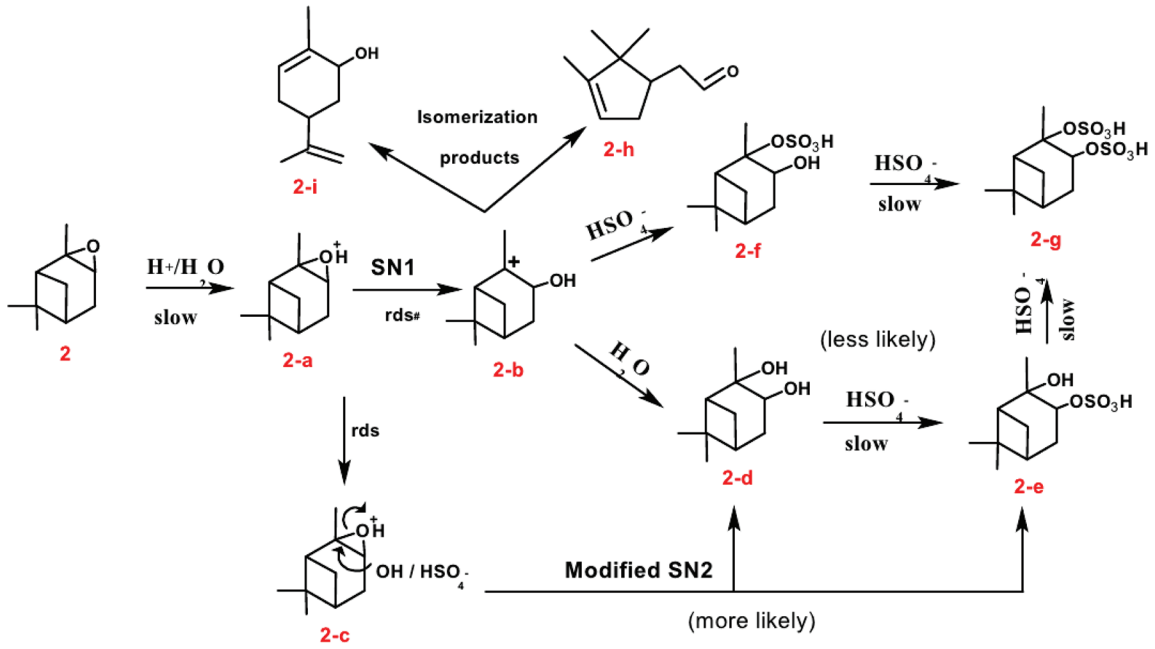

lower volatility. Because the rate constants of the acetal formation and aldol condensation reactions are positively correlated with temperature,[72,73] at lower temperatures these reactions become less favorable. As a result, aldehydes and hydroxy-alkenes evaporate from sulfuric acid solution rather than form low volatility products.

The products remaining in the condensed phase were identified from the spectroscopic experiments using ATR-FTIR. At high RH conditions, absorbance peaks for both primary and tertiary alcohol groups are observed. From this observations and with reference to a previous study,[39] the structure of the diol formed is inferred to be 1,2-hydroxy isoprene. The presence of other diol structure is difficult to confirm solely from the ATR-FTIR spectrum. With decreasing humidity (i.e., increasing acidity), acetal formation is observed, which leads to increased absorbance intensities for the C−H and C−O−C stretches and decreased O−H vibrations. The increase in number of C−O−C groups due to acetal formation leads to increased absorbance for the C−H peaks relative to that for C−OH.

In contrast to the observations made in the study by Eddingsaas et al.,[40] where sulfate ester was detected in the reaction of *cis*-2,3-epoxybutane-1,4-diol with 1 M H_2SO_4 solution, no sulfate ester is formed in case of isoprene epoxide at a similar acid concentration. This can be explained by the high acid hydrolysis reaction rate coefficient of isoprene epoxide, as reported by Minerath et al.[39] As a result, hydrolysis proceeds much faster than esterification and no organosulfate is formed. On the contrary, in epoxides with hydroxy substituents, such as *cis*-2,3-epoxybutane-1,4-diol, the hydrolysis rate is reduced because the presence of hydroxyl group stabilizes the carbocation, making it more available for the nucleophilic attack, thus favoring organosulfate formation.

In the NMR studies, 1,2-diols, 1,4-diols, and aldehydes are identified in all experiments. Aldehyde formation is generally unexpected at low acid concentrations. The formation of aldehydes in the NMR experiments is therefore attributed to the kinetic isotope effect (KIE), which can be quantitatively expressed as the ratio of isotopic rate constants (k_H/k_D).[74] For a rate-limiting step of a chemical reaction, the isotope substitution of atoms involved in a bond formation or cleavage greatly modifies the reaction rate,[75,76] and the isotope effect for the hydrogen−deuterium replacements in particular is large due to the exclusive mass relation between the two isotopes.[74] The use of deuterated solvent (D_2O) and the reactant (D_2SO_4) can therefore result in large KIE for the rate-limiting step. Also, because KIE is often significantly larger for SN1 reactions as compared to the SN2 reactions,[77] aldehyde formation via SN1 pathway is facilitated. The absence of the acetal signal in the NMR experiments is caused by low concentrations of aldehyde and acid, compared to those in the ATR-FTIR experiments, to support efficient acetal formation. Aldehydes are not observed in ATR-FTIR experiments because of the faster reaction of aldehydes to form acetals at high acidity.

4.2. α-Pinene Oxide. The proposed mechanism of acid catalyzed hydrolysis reaction of α-pinene oxide is illustrated in Scheme 2. The protonated epoxide (2-a) undergoes either an SN1 mechanism (via 2-b) or modified SN2 mechanism (via 2-c) to form different products. In the acid hydrolysis of α-pinene oxide, both diol and sulfate esters are formed, in contrast to that for isoprene oxide. Diol is found to be the major product at low acid concentrations. Sulfate esters are formed at high acid concentrations, either by esterification of the alcohol group or by direct attack of HSO_4^- nucleophile on the intermediate (2-b/2-c). Several previous studies have shown formation of sulfate esters in the reaction of epoxides with sulfuric acid[14,37,38] and by esterification of alcohols.[36] However, the latter reaction is slow and may have contributed negligibly to the organosulfate production in our experiments. Some isomerization products (2-i/2-h) are also expected to form by rearrangement of intermediate 2-b or by the dehydration of diol (2-d) in the presence of acid. These isomerization products are inferred from ID-CIMS experiments and directly observed in NMR experiments. However, there is no evidence that any condensation products such as aldol or acetal are formed in acid catalyzed reaction of α-pinene oxide.

According to the ID-CIMS experiments, the heterogeneous reaction of α-pinene oxide with 90 wt % H_2SO_4 is irreversible at 298 K, similar to isoprene oxide. The uptake coefficient for

dx.doi.org/10.1021/jp2112704 | J. Phys. Chem. A 2012, 116, 6078−6090

α-pinene oxide is by a factor of ~3 larger than that for isoprene oxide. This may be explained by either a higher reactivity of α-pinene oxide or by lower interference from its reaction products. At lower temperatures, significant interference is observed, and as for isoprene oxide, the volatile products are inferred to be either aldehyde (2-h) or hydroxy-alkene (2-i). The structures of these compounds have been proposed in a previous study,[37] where it has been shown that isomerization reactions most likely compete with the nucleophilic attack at the tertiary carbon atom. According to the study on sulfate esterification by Minerath et al.,[36] due to high activation energy, the sulfate ester formation is not favorable at lower temperatures. Thus, at higher temperatures, sulfate esters form and stay in solution, owing to their low vapor pressure. At lower temperatures, the aldehyde or hydroxy-alkene preferably forms and then evaporates from condensed phase, interfering with the detection of α-pinene oxide.

Spectroscopic studies using ATR-FTIR reveal the formation of organosulfates at high acid concentrations, that is, at low RH. No rearrangement products are observed in these experiments as confirmed from the absence of functional groups like C═O and C═C in the spectra. Condensation products such as aldol or acetal do not form in case of α-pinene oxide. The yield of organosulfates decreases with decreasing acidic sulfate concentration, and at RH greater than 40%, the acid concentration is too low to support any organosulfate production. At high RH conditions, the absorption features of secondary and tertiary alcohol groups are identified, confirming that the diol formed is 2-d. The structures of organosulfates inferred from the reaction mechanisms of epoxides and alcohols are in agreement with those from the previous studies.[36,37]

Figure 6 shows the integrated C−H stretch absorbance over time as a function of RH. The slope of absorbance increases with increasing RH, in contrast to that observed for isoprene oxide, where the slope of C−H absorbance decreases with increasing RH. These observations can be attributed to the different mechanisms and different products formed under low RH conditions for the two epoxides. The difference in reactivity at high and low RH is also supported by the optical microscopic images of H_2SO_4 microdroplets exposed to α-pinene epoxide, as shown in Figure 7. The sulfuric acid droplets are seen to lose their identity and spread out on the surface in a layer at high RH, while they stay intact at low RH conditions. The spreading is observed only when the acid is exposed to epoxide at high humidities. In absence of epoxide, the spreading does not occur at similarly high humidity. Also, the spreading features show patterns of light interference, indicating that the film thickness is comparable with the light wavelength, that is, ~500 nm. Apparently, the organic reaction products act as surfactants to decrease the contact angle of microdroplets with the crystal, resulting in a thin film. At low RH conditions, due to low water activity hydrolysis is suppressed. On the contrary, organosulfate formation is facilitated at low RH conditions, and therefore, loss of O−H absorbance corresponding to H_2SO_4 is evident in the spectra.

In the NMR experiments, 2-pinanol-3-hydrogen sulfate product (2-e) is found to be preferably formed, with the sulfate group attached to the less sterically hindered carbon atom. This product can be produced either by esterification of diol (2-d) or directly from intermediate 2-c by a modified SN2 mechanism, which is more likely to occur. With increasing acidity, the polar and hyperconjugative effects of the methyl group start playing a role by overcoming the steric effects and leading to more formation of hydroxy-sulfate with sulfate group attached to the tertiary carbon atom.[66] Hence, the ratio of 3-pinanol-2-hydrogen sulfate (2-f) to 2-pinanol-3-hydrogen sulfate (2-e) is evident to increase with increasing acidity. Also, with increasing acidity and, hence, molar concentration of sulfate, diester products are formed. The earlier studies have shown that the yield of sulfate ester formed by acid-catalyzed reactions of epoxides depends on sulfate concentration but not on $[H^+]$.[38−40] The observations in this study are consistent with those studies, showing the dependency of sulfate ester yield on available acidic sulfate (Figure 8). With respect to diol formation, the NMR results obtained in this study are in agreement with the ATR-FTIR results, showing that diols are formed primarily at low acid concentrations. Formation of organosulfate in NMR studies with 5 wt % acid and absence of organosulfate at the same acid concentration in ATR-FTIR studies is attributed to KIE. Different products formed from these common intermediates 2-b and 2-c are likely to exhibit different individual KIE and the competition between these product formation pathways can lead to an overall enhanced KIE for the route leading to organosulfate.[75,76] Also, the unusually high KIE observed for reactions of epoxides in D_2SO_4/D_2O may indicate tunneling behavior,[75] and explain the formation of diester products, which have not been reported earlier.

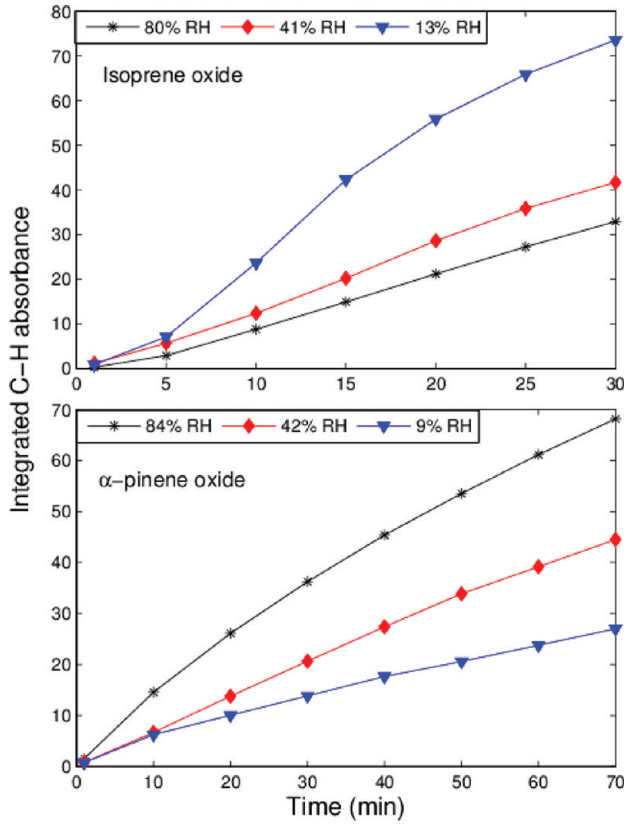

Figure 6. Integrated absorbance for the C−H stretch region (3000−2850 cm^{-1}) over time for isoprene oxide and α-pinene oxide at different RH.

5. ATMOSPHERIC IMPLICATIONS

From our laboratory measurements of the uptake and analysis of reaction products for the two epoxides at different acid concentrations and temperatures, we evaluate the contribution of heterogeneous chemistry to the removal of gas-phase epoxides and to the growth of SOA in the atmosphere. For a

dx.doi.org/10.1021/jp2112704 | J. Phys. Chem. A 2012, 116, 6078−6090

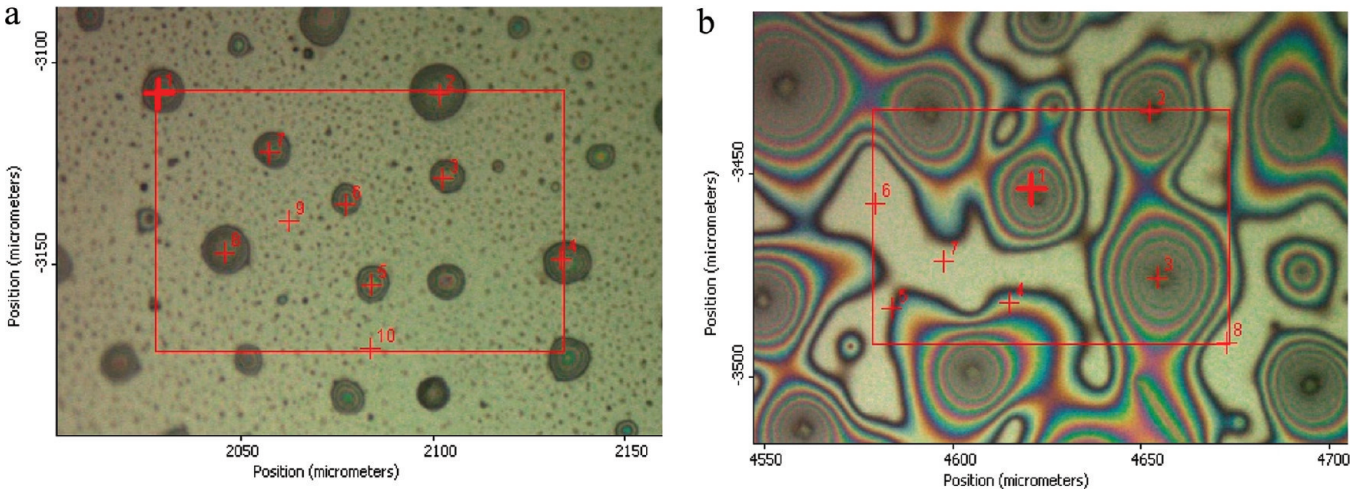

Figure 7. Optical microscopic images of a silicon wafer chip with H_2SO_4 microdroplets exposed to 2.1×10^{14} molecules cm^{-3} α-pinene oxide at (a) 9% RH and (b) 84% RH.

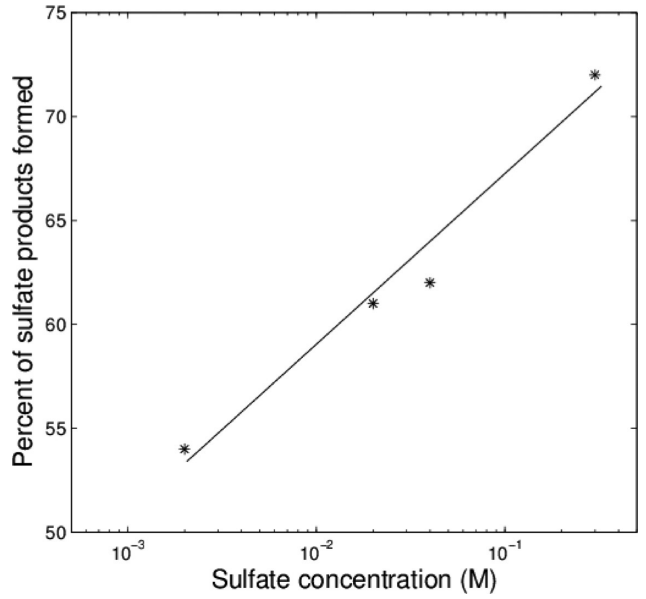

Figure 8. Sulfate ester product yield dependence as a function of available inorganic acidic sulfate in solution.

sulfuric acid aerosol population with a total surface area of 5×10^2 μm^2 cm^{-3}, corresponding to ~10 μg m^{-3} mass loading, the lifetimes of isoprene epoxide and α-pinene oxide with respect to heterogeneous loss are 30 and 15 min, respectively. The lifetime for a heterogeneous reaction can be compared to those for the gas-phase oxidation of epoxides by OH and O_3. Taking the global concentration of OH (10^6 molecules cm^{-3}) and O_3 (10^{12} molecules cm^{-3}),[78] and assuming a rate constant close to that for vinyl ethers,[79,80] the lifetime of isoprene oxide against OH is estimated to be 3−6 h and against O_3 > 1 day. α-Pinene oxide, because of the absence of double bonds, is not expected to react with ozone. Its lifetime against OH is estimated to be several hours, assuming a reactivity similar to that of a proxy, cyclic ether 1,8-cineole.[81−83] These estimates suggest that heterogeneous reactions on acidic aerosols are faster and more efficient than gaseous reactions with atmospheric oxidants and hence may represent the major removal pathway for epoxides.

Our measured uptake coefficients suggest that the heterogeneous reaction between the epoxides and acidic sulfate aerosols is fast and can contribute to SOA formation and growth. An upper limit for the growth rates of isoprene oxide and α-pinene oxide is estimated to be 15 and 53 nm hr^{-1}, respectively, for a 1 ppb of the epoxide, assuming that all products remain in the particle phase and neglecting the Kelvin effect. These growth rates and the lifetimes of epoxides indicate that for acidic particles at warmer tropospheric temperatures, the heterogeneous reactions of epoxides take place efficiently. Ambient measurements have shown that in urban environment, particle acidity can be significantly high, with pH varying in the range of 0−5.[84] Epoxides can react rapidly in this pH range and some of the products formed by the heterogeneous reactions are of low volatility and, hence, can contribute to SOA particle growth. These organic products can modify both the chemical and physical properties of aerosol particles, thus affecting their radiative and cloud forming properties. In dilute acidic aerosols, the reactivity of the two epoxides is reduced or the products formed are of relatively high volatility that evaporate readily to the gas phase. Thus, although slightly acidic aerosols can act as a heterogeneous medium for conversion of gas-phase epoxides to gas-phase hydrolysis products, such a process may contribute negligibly to the size growth.

6. CONCLUSIONS

This study represents an extensive laboratory investigation of the heterogeneous reactions of isoprene oxide and α-pinene oxide with sulfuric acid, ammonium bisulfate, and ammonium sulfate. The uptake experiments using ID-CIMS show that the heterogeneous uptake of both epoxides on sulfuric acid is fast and irreversible, with a temperature-dependent reaction mechanism. Volatile products like aldehydes and monohydroxyalkenes are formed at lower temperatures, while polyhydroxy products, organosulfates, and condensation products such as aldol and acetal are formed at room temperature in the acid hydrolysis of epoxides. The spectroscopic studies using ATR-FTIR reveal that at high RH (i.e., at low acid concentration) both isoprene oxide and α-pinene oxide form diols. With increasing acid concentration, sulfate ester formation is facilitated for α-pinene oxide, while acetal formation is preferred for isoprene oxide. Although organosulfate formation has been observed earlier for α-pinene oxide,[37] the formation of acetal is reported here for the first time. Both of these low vapor

pressure products, acetals and organosulfates, can contribute to SOA growth in the atmosphere. Irrespective of the RH condition, the amount of organics formed is proportional to epoxide concentration, thus following the first-order reaction with respect to epoxide concentration. The importance of acid catalysis for uptake of epoxides is justified by absence of any product in reaction with ammonium sulfate. In the NMR studies, formation of diols and organosulfates is observed, complementing the results from ATR-FTIR experiments. Similar products formed in NMR experiments at very low acid concentrations compared to that used in experiments with other techniques indicate the presence of KIE. Aldehyde formation from isoprene oxide is significantly faster in D_2O than in H_2O at low acid concentration and it is observable in NMR spectra because subsequent acetal formation is slow. Some dehydration products are also observed for both epoxides, in agreement with previously proposed acid catalyzed reaction mechanisms of epoxides.[37,66] It should be pointed out that the epoxide hydrolysis rate constants measured in deuterated solutions by NMR may not be applicable to atmospheric evaluations because of the strong effect of KIE on the reaction mechanism and the rates of individual pathways.

It can be concluded from our study that the reaction mechanism and products of isoprene oxide and α-pinene oxide depend on the acid concentration, amount of water in aerosol, and temperature. This can also be expected for other epoxides, thus, showing that, under favorable conditions, epoxides can be very efficient SOA precursors. These conditions include urban atmospheres where warmer temperatures and higher SO_2 concentrations are expected. It is clear that even the highly volatile isoprene oxide can contribute to SOA formation and growth efficiently. However, further research is required to obtain a better understanding of the reactivity of epoxides and to quantify reaction products at lower temperatures. Other epoxides are also needed to be investigated to identify the effect of electron donor and electron acceptor substituents on the epoxide reactivity as well as distributions and properties of organic products that could potentially contribute to SOA growth. Furthermore, future studies are needed to investigate the acid-catalyzed reaction of epoxides in the presence of other organic compounds, which may potentially increase the yield of low volatility products formed.

AUTHOR INFORMATION

Corresponding Author

*E-mail: renyi-zhang@tamu.edu.

Notes

The authors declare no competing financial interest.

ACKNOWLEDGMENTS

This work was supported by the Robert A. Welch Foundation (Grant A-1417) and the National Science Foundation (AGS-0938352). The authors thank Sarah Brooks for the use of an optical microscope.

REFERENCES

(1) Ravishankara, A. R. *Science* **1997**, *276*, 1058−1065.
(2) Atkinson, R.; Arey, J. *Chem. Rev.* **2003**, *103*, 4605−4638.
(3) Lei, W. F.; Zhang, R. Y. *J. Phys. Chem. A* **2001**, *105*, 3808−3815.
(4) Zhang, D.; Lei, W. F.; Zhang, R. Y. *Chem. Phys. Lett.* **2002**, *358*, 171−179.
(5) Kroll, J. H.; Seinfeld, J. H. *Atmos. Environ.* **2008**, *42*, 3593−3624.
(6) Hallquist, M.; Wenger, J. C.; Baltensperger, U.; Rudich, Y.; Simpson, D.; Claeys, M.; Dommen, J.; Donahue, N. M.; George, C.; Goldstein, A. H.; et al. *Atmos. Chem. Phys.* **2009**, *9*, 5155−5236.
(7) Forster, P.; Ramaswamy, V.; Artaxo, P.; Berntsen, T.; Betts, R.; Fahey, D. W.; Haywood, J.; Lean, J.; Lowe, D. C.; Myhre, G. et al. Changes in Atmospheric Constituents and in Radiative Forcing. In *Climate Change 2007: The Physical Science Basis. Contribution of Working Group I to the Fourth Assessment Report of the Intergovernmental Panel on Climate Change*; Solomon, S., Qin, D., Manning, M., Chen, Z., Marquis, M., Averyt, K. B., Tignor, M., Miller, H. L., Eds.; Cambridge University Press: Cambridge, United Kingdom and New York, NY, 2007.
(8) Li, G.; Zhang, R.; Fan, J.; Tie, X. *J. Geophys. Res.* **2005**, *110*, D23206, DOI: 10.1029/2005JD005898.
(9) Zhang, R. Y.; Li, G. H.; Fan, J. W.; Wu, D. L.; Molina, M. J. *Proc. Natl. Acad. Sci. U.S.A.* **2007**, *104*, 5295−5299.
(10) Pankow, J. F.; Seinfeld, J. H.; Asher, W. E.; Erdakos, G. B. *Environ. Sci. Technol.* **2001**, *35*, 1164−1172.
(11) Donahue, N. M.; Robinson, A. L.; Stanier, C. O.; Pandis, S. N. *Environ. Sci. Technol.* **2006**, *40*, 2635−2643.
(12) Levitt, N. P.; Zhao, J.; Zhang, R. Y. *J. Phys. Chem. A* **2006**, *110*, 13215−13220.
(13) Zhao, J.; Levitt, N. P.; Zhang, R.; Chen, J. *Environ. Sci. Technol.* **2006**, *40*, 7682−7687.
(14) Iinuma, Y.; Müller, C.; Berndt, T.; Böge, O.; Claeys, M.; Herrmann, H. *Environ. Sci. Technol.* **2007**, *41*, 6678−6683.
(15) Wang, L.; Khalizov, A. F.; Zheng, J.; Xu, W.; Ma, Y.; Lal, V.; Zhang, R. *Nature Geosci.* **2010**, *3*, 238−242.
(16) Wang, L.; Xu, W.; Khalizov, A. F.; Zheng, J.; Qiu, C.; Zhang, R. *J. Phys. Chem. A* **2011**, *115*, 8940−8947.
(17) Zhang, R. Y.; Suh, I.; Zhao, J.; Zhang, D.; Fortner, E. C.; Tie, X. X.; Molina, L. T.; Molina, M. J. *Science* **2004**, *304*, 1487−1490.
(18) Fan, J. W.; Zhang, R. Y.; Collins, D.; Li, G. H. *Geophys. Res. Lett.* **2006**, *33*, L15802.
(19) Zhang, R.; Wang, L.; Khalizov, A. F.; Zhao, J.; Zheng, J.; McGraw, R. L.; Molina, L. T. *Proc. Natl. Acad. Sci. U.S.A.* **2009**, *106*, 17650−17654.
(20) Zhao, J.; Khalizov, A.; Zhang, R.; McGraw, R. *J. Phys. Chem. A* **2009**, *113*, 680−689.
(21) Zhang, R.; Khalizov, A.; Wang, L.; Hu, M.; Xu, W. *Chem. Rev.* **2012**, *112*, DOI: 10.1021/cr2001756.
(22) Guenther, A.; Karl, T.; Harley, P.; Wiedinmyer, C.; Palmer, P. I.; Geron, C. *Atmos. Chem. Phys.* **2006**, *6*, 3181−3210.
(23) Henze, D. K.; Seinfeld, J. H. *Geophys. Res. Lett.* **2006**, *33*, L09812.
(24) Henze, D. K.; Seinfeld, J. H.; Ng, N. L.; Kroll, J. H.; Fu, T. M.; Jacob, D. J.; Heald, C. L. *Atmos. Chem. Phys.* **2008**, *8*, 2405−2420.
(25) Surratt, J. D.; Lewandowski, M.; Offenberg, J. H.; Jaoui, M.; Kleindienst, T. E.; Edney, E. O.; Seinfeld, J. H. *Environ. Sci. Technol.* **2007**, *41*, 5363−5369.
(26) Surratt, J. D.; Kroll, J. H.; Kleindienst, T. E.; Edney, E. O.; Claeys, M.; Sorooshian, A.; Ng, N. L.; Offenberg, J. H.; Lewandowski, M.; Jaoui, M.; et al. *Environ. Sci. Technol.* **2007**, *41*, 517−527.
(27) Surratt, J. D.; Gómez-González, Y.; Chan, A. W. H.; Vermeylen, R.; Shahgholi, M.; Kleindienst, T. E.; Edney, E. O.; Offenberg, J. H.; Lewandowski, M.; Jaoui, M.; et al. *J. Phys. Chem. A* **2008**, *112*, 8345−8378.
(28) Iinuma, Y.; Muller, C.; Berndt, T.; Boge, O.; Claeys, M.; Herrmann, H. *Environ. Sci. Technol.* **2007**, *41*, 6678−6683.
(29) Gomez-Gonzalez, Y.; Surratt, J. D.; Cuyckens, F.; Szmigielski, R.; Vermeylen, R.; Jaoui, M.; Lewandowski, M.; Offenberg, J. H.; Kleindienst, T. E.; Edney, E. O.; et al. *J. Mass Spectrom.* **2008**, *43*, 371−382.
(30) Chan, M. N.; Surratt, J. D.; Claeys, M.; Edgerton, E. S.; Tanner, R. L.; Shaw, S. L.; Zheng, M.; Knipping, E. M.; Eddingsaas, N. C.; Wennberg, P. O.; et al. *Environ. Sci. Technol.* **2010**, *44*, 4590−4596.
(31) Froyd, K. D.; Murphy, S. M.; Murphy, D. M.; de Gouw, J. A.; Eddingsaas, N. C.; Wennberg, P. O. *Proc. Natl. Acad. Sci. U.S.A.* **2010**, *107*, 21360−21365.

(32) Olson, C. N.; Galloway, M. M.; Yu, G.; Hedman, C. J.; Lockett, M. R.; Yoon, T.; Stone, E. A.; Smith, L. M.; Keutsch, F. N. *Environ. Sci. Technol.* **2011**, *45*, 6468−6474.
(33) Hatch, L. E.; Creamean, J. M.; Ault, A. P.; Surratt, J. D.; Chan, M. N.; Seinfeld, J. H.; Edgerton, E. S.; Su, Y. X.; Prather, K. A. *Environ. Sci. Technol.* **2011**, *45*, 8648−8655.
(34) Hatch, L. E.; Creamean, J. M.; Ault, A. P.; Surratt, J. D.; Chan, M. N.; Seinfeld, J. H.; Edgerton, E. S.; Su, Y. X.; Prather, K. A. *Environ. Sci. Technol.* **2011**, *45*, 5105−5111.
(35) Lin, Y.-H.; Zhang, Z.; Docherty, K. S.; Zhang, H.; Budisulistiorini, S. H.; Rubitschun, C. L.; Shaw, S. L.; Knipping, E. M.; Edgerton, E. S.; Kleindienst, T. E.; et al. *Environ. Sci. Technol.* **2011**, *46*, 250−258.
(36) Minerath, E. C.; Casale, M. T.; Elrod, M. J. *Environ. Sci. Technol.* **2008**, *42*, 4410−4415.
(37) Iinuma, Y.; Boge, O.; Kahnt, A.; Herrmann, H. *Phys. Chem. Chem. Phys.* **2009**, *11*, 7985−7997.
(38) Minerath, E. C.; Elrod, M. J. *Environ. Sci. Technol.* **2009**, *43*, 1386−1392.
(39) Minerath, E. C.; Schultz, M. P.; Elrod, M. J. *Environ. Sci. Technol.* **2009**, *43*, 8133−8139.
(40) Eddingsaas, N. C.; VanderVelde, D. G.; Wennberg, P. O. *J. Phys. Chem. A* **2010**, *114*, 8106−8113.
(41) Darer, A. I.; Cole-Filipiak, N. C.; O'Connor, A. E.; Elrod, M. J. *Environ. Sci. Technol.* **2011**, *45*, 1895−1902.
(42) Alvarado, A.; Tuazon, E. C.; Aschmann, S. M.; Atkinson, R.; Arey, J. *J. Geophys. Res.* **1998**, *103*, 25541−25551.
(43) Atkinson, R.; Arey, J.; Aschmann, S.; Tuazon, E. *Res. Chem. Intermed.* **1994**, *20*, 385−394.
(44) Atkinson, R.; Aschmann, S. M.; Arey, J.; Tuazon, E. C. *Int. J. Chem. Kinet.* **1994**, *26*, 945−950.
(45) Skov, H.; Benter, T.; Schindler, R. N.; Hjorth, J.; Restelli, G. *Atmos. Environ.* **1994**, *28*, 1583−1592.
(46) Benter, T.; Liesner, M.; Schindler, R. N.; Skov, H.; Hjorth, J.; Restelli, G. *J. Phys. Chem.* **1994**, *98*, 10492−10496.
(47) Berndt, T.; Boge, O. *Int. J. Chem. Kinet.* **1997**, *29*, 755−765.
(48) Berndt, T.; Boge, O. *J. Chem. Soc., Faraday Trans.* **1997**, *93*, 3021−3027.
(49) Paulot, F.; Crounse, J. D.; Kjaergaard, H. G.; Kurten, A.; Clair, J. M. St; Seinfeld, J. H.; Wennberg, P. O. *Science* **2009**, *325*, 730−733.
(50) Surratt, J. D.; Chan, A. W. H.; Eddingsaas, N. C.; Chan, M.; Loza, C. L.; Kwan, A. J.; Hersey, S. P.; Flagan, R. C.; Wennberg, P. O.; Seinfeld, J. H. *Proc. Natl. Acad. Sci. U.S.A.* **2010**, *107*, 6640−6645.
(51) Wang, L.; Lal, V.; Khalizov, A. F.; Zhang, R. *Environ. Sci. Technol.* **2010**, *44*, 2461−2465.
(52) Qiu, C.; Wang, L.; Lal, V.; Khalizov, A. F.; Zhang, R. *Environ. Sci. Technol.* **2011**, *45*, 4748−4755.
(53) Molina, M. J.; Molina, L. T.; Zhang, R. Y.; Meads, R. F.; Spencer, D. D. *Geophys. Res. Lett.* **1997**, *24*, 1619−1622.
(54) Zhang, R. Y.; Leu, M. T.; Molina, M. J. *Geophys. Res. Lett.* **1996**, *23*, 1669−1672.
(55) Zhang, D.; Zhang, R. *Environ. Sci. Technol.* **2005**, *39*, 5722−5728.
(56) Zhang, R.; Wooldridge, P. J.; Abbatt, J. P. D; Molina, M. J. *J. Phys. Chem.* **1993**, *97*, 7351−7358.
(57) Zhang, R. Y.; Wooldridge, P. J.; Molina, M. J. *J. Phys. Chem.* **1993**, *97*, 8541−8548.
(58) Molina, M. J.; Zhang, R.; Wooldridge, P. J.; McMahon, J. R.; Kim, J. E.; Chang, H. Y.; Beyer, K. D. *Science* **1993**, *261*, 1418−1423.
(59) Schoon, N.; Amelynck, C.; Vereecken, L.; Coeckelberghs, H.; Arijs, E. *Int. J. Mass Spectrom.* **2004**, *239*, 7−16.
(60) Green, D. W.; Perry, R. H. *Perry's Chemical Engineers' Handbook*, 8th ed.; McGraw-Hill: New York, 2008.
(61) Tang, I. N.; Munkelwitz, H. R. *J. Geophys. Res.* **1994**, *99*, 18801−18808.
(62) Bryan, W. P.; Byrne, R. H. *J. Chem. Educ.* **1970**, *47*, 361.
(63) Qiu, C.; Wang, L.; Lal, V.; Khalizov, A. F.; Zhang, R. *Environ. Sci. Technol.* **2011**.
(64) Socrates, G. *Infrared and Raman Characteristic Group Frequencies: Tables and Charts*, 3rd ed.; Wiley: Chichester; New York, 2001.
(65) Gilardoni, S.; Russell, L. M.; Sorooshian, A.; Flagan, R. C.; Seinfeld, J. H.; Bates, T. S.; Quinn, P. K.; Allan, J. D.; Williams, B.; Goldstein, A. H.; et al. *J. Geophys. Res.* **2007**, *112*, D10S27.
(66) Parker, R. E.; Isaacs, N. S. *Chem. Rev.* **1959**, *59*, 737−799.
(67) Whalen, D. L. Mechanisms of hydrolysis and rearrangements of epoxides. In *Advances in Physical Organic Chemistry*; Richard, J. P., Ed.; Academic Press: New York, 2005; Vol. *40*; pp 247−298.
(68) Ley, J. B.; Vernon, C. A. *J. Chem. Soc.* **1957**, 2987−2993.
(69) Clark, D. J.; Williams, G. *J. Chem. Soc.* **1957**, 4218−4221.
(70) Španěl, P.; Doren, J. M. V.; Smith, D. *Int. J. Mass Spectrom.* **2002**, *213*, 163−176.
(71) Zhao, J.; Zhang, R. Y. *Atmos. Environ.* **2004**, *38*, 2177−2185.
(72) Kormanovskaya, G. N.; Vlodavets, I. N. *Izv. Akad. Nauk SSSR, Ser. Khim.* **1965**, 737−739.
(73) Casale, M. T.; Richman, A. R.; Elrod, M. J.; Garland, R. M.; Beaver, M. R.; Tolbert, M. A. *Atmos. Environ.* **2007**, *41*, 6212−6224.
(74) Limbach, H. H. Dynamic NMR Spectroscopy in the Presence of Kinetic Hydrogen/Deuterium Isotope Effects. In *NMR-Basic Principles and Progress*; Diehl, P., Fluck, E., Ed.; Springer: Heidelberg, 1991; Vol. *23*; pp 63−164.
(75) Thibblin, A. *J. Phys. Org. Chem.* **1988**, *1*, 161−167.
(76) Thibblin, A.; Ahlberg, P. *Chem. Soc. Rev.* **1989**, *18*, 209−224.
(77) Pocker, Y.; Ronald, B. P.; Anderson, K. W. *J. Am. Chem. Soc.* **1988**, *110*, 6492−6497.
(78) Seinfeld, J. H.; Pandis, S. N. *Atmospheric Chemistry and Physics - From Air Pollution to Climate Change*, 2nd ed.; John Wiley & Sons: New York, 2006.
(79) Al Mulla, I.; Viera, L.; Morris, R.; Sidebottom, H.; Treacy, J.; Mellouki, A. *ChemPhysChem* **2010**, *11*, 4069−4078.
(80) Zhou, S.; Barnes, I.; Zhu, T.; Bejan, I.; Benter, T. *J. Phys. Chem. A* **2006**, *110*, 7386−7392.
(81) Atkinson, R.; Arey, J. *Atmos. Environ.* **2003**, *37*, 197−219.
(82) Corchnoy, S. B.; Atkinson, R. *Environ. Sci. Technol.* **1990**, *24*, 1497−1502.
(83) Atkinson, R.; Hasegawa, D.; Aschmann, S. M. *Int. J. Chem. Kinet.* **1990**, *22*, 871−887.
(84) Zhang, Q.; Jimenez, J. L.; Worsnop, D. R.; Canagaratna, M. *Environ. Sci. Technol.* **2007**, *41*, 3213−3219.